LA-UR-19-26595
Approved for public release; distribution is unlimited.

Title: Interim Report on the Experimental Evaluation of the Fast-Neutron Passive Collar (FNPC) Performance

Author(s): Menlove, Howard Olsen
Geist, William H.
Root, Margaret A.

Intended for: Report

Issued: 2019-07-12

Interim Report on the Experimental Evaluation of the Fast-Neutron Passive Collar (FNPC) Performance

Howard Menlove, William Geist, and Margaret Root

Los Alamos National Laboratory, Group NEN-1

1. Background

This report represents a deliverable in the Safeguards Technology WBS # Project Title, 24.1.3.1, Task 3 (Report on laboratory-based performance testing of the FNPC).

A new, simplified method for the verification of the ^{235}U mass in fresh LEU fuel assemblies that is relatively independent of burnable poison content is being developed. LWR fresh fuel is currently verified using the uranium neutron coincidence collar (UNCL) [1], which relies on an AmLi source to induce fission in the ^{235}U. AmLi neutrons are slowed down in polyethylene, so the induced fission is primarily due to thermal neutrons. Burnable poisons, which are added to nuclear fuel assemblies to extend the lifetime of the fuel, absorb neutrons that would otherwise have induced fission in the fuel, thereby reducing the neutron count rate and thus the measured ^{235}U mass. To remove this bias factor a correction is applied based on the operator's declared burnable poison content.

The new technique uses ^{238}U spontaneous fission in LWR fresh fuel rods to self-interrogate the ^{235}U mass. The ^{238}U spontaneous fission neutrons have a hard neutron energy spectrum, which means that the technique is less sensitive to burnable poisons than the AmLi based systems. This project has continued the work done over the past two years to study this new technique using the optimized ^{3}He based fast-neutron passive collar (FNPC). Fabrication of the FNPC has been completed and measurements are in progress using the LANL mockup PWR fuel assembly. Also, preliminary evaluations of advanced analysis techniques and unattended mode operation have been performed.

In FY18, the ^{3}He tube based detector was compared with a ^{10}B sealed cell based detector for the same set of PWR fuel assemblies in the Rodeo-II program [2]. The results were that the optimized ^{3}He detector had higher efficiency and less weight than the ^{10}B based system where both systems had about the same cost. Thus, the FY19 work continued exclusively with the ^{3}He based detector; although, either system had the potential for future applications. However, the high efficiency of the FPNC (~24%) is critical for precise measurements of the triples rate necessary in the multiplicity advanced analysis technique which can solve for the burnable poison content.

2. Concept

The concept for the new technique is that the combined spontaneous fission and the induced fission reactions in the fuel emits a boosted effective average number of neutrons ($\bar{\nu}$) that is a combination of $\bar{\nu}$ (spontaneous fission) = 2.07 and $\bar{\nu}$ (induced fission) = 2.44. This higher effective multiplicity provides an increase in the net coincident signal from the ^{235}U compared with the spontaneous fission reactions from the ^{238}U. Also, as the ^{235}U enrichment increases in the fuel pellets, the ^{234}U (α,n) neutron emission rate increases the observed neutron emission rate. The hard energy spectrum and the increase in the neutrons

with enrichment result in a more linear calibration functions for the measured single, doubles, and triples rates than with the standard UNCL. The high efficiency of the new detector and the low background counting rates provides triples rates with useable statistical precision in measurement times of about 600s. The availability of the singles, doubles, and triples makes multiplicity counting and advanced analysis possible to determine both the ^{235}U and the burnable poison loadings. The "advanced analysis" concept for active neutron interrogation has been documented in a prior paper [3].

3. Passive Neutron Collar Design and Hardware Status

The optimization of the FNPC detector slabs was completed in FY18, and the final MCNP based design is shown in Fig. 1 [4]. There are 28 ^{3}He tubes with 6 bar pressure. The size and weight are approximately the same as the current UNCL that is in use by the IAEA. One of the detector slabs for the passive collar is shown in Fig. 2 where the new junction box design by PDT is compact allowing an additional 10 cm of active length to the 3He tubes while keeping the total height the same as for the current UNCL. The V notch in the front and back slabs shown in Fig.1 are to accommodate the size of the hexagonal WWER-1000 fuel assemblies. There is a HDPE filler piece that is used for PWR assemblies.

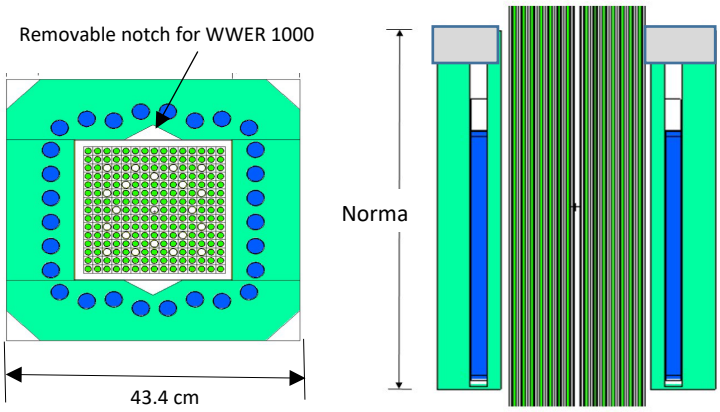

Fig. 1. The MCNP design for the optimized FNPC based on 3He tubes

One of the detector slabs with the ^{3}He tubes and the PDT junction box is shown in Fig. 2 where the Reuter-Stokes ^{3}He tubes are described in Table 1. The ^{3}He tubes screw directly into the new junction box (JB) without opening the lid, so that the tubes are easily removable. The JB is only 3.5 cm deep and contains one PDT amplifier to service the 6 or 8 tubes. The thin JB design allowed for the additional 10 cm of active length for the tubes compared with prior UNCL designs (i.e. 17" vs. 13") [1]. All HV connections are hermetically sealed to be moisture resistant.

Table 1. Detector tube specifications for the FNPC

Tube Model	RS-P4-0817-104
Admixture	$ArCH^4$
Number	28
Gas pressure	6 bar
Cathode	Al
Operating Bias	1260 V

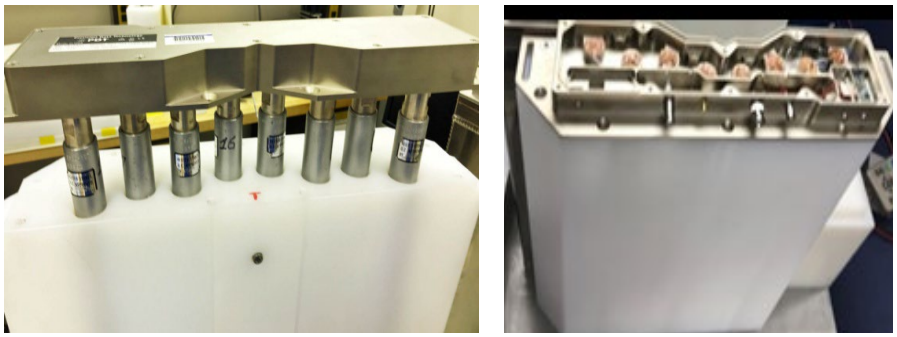

Fig. 2. The ^{3}He tubes in the HDPE moderator with the WWER-1000 notch filler (left), and the open JB (right) with the epoxy sealer in the HV connections for each of the 8 tubes.

The complete FNPC is shown in Fig. 3 where it is assembled around the LANL mockup 15x15 rod PWR fuel assembly. The front slab on the detector is a door that is hinged (see Fig.3 right) to allow fuel assembly insertion through the front of the collar as well as from above.

Fig. 3. The complete collar system that surrounds the LANL mockup fuel assembly where hinges for the removable door are shown (right).

The electronics to support the FPNC are the shift register JSR-15 [5], the optional advanced list mode module (ALMM) [6], and a laptop computer as shown in Fig.4. The alternative data collection with the list mode ALMM is being investigated as a more sensitive tool for cosmic-ray spallation rejection in the background. These same electronic modules are in use by the IAEA for the current UNCL and other fielded instruments.

Fig. 4. The electronics for data collection and signal processing are shown with the ALMM (left) and the JSR-15 (right).

4. Experimental Characterization for the Detector

Experiments were performed to check for electronic noise, to gain match the four slabs of the FNPC, and to determine the optimum operating parameters for the system.

4.1 Plateau Curves

To check for noise and to gain match the detector slabs a ^{252}Cf source in the center of the empty detector was measured while the HV was varied from 900 V to 1400 V in 20 V steps and the results are shown in Fig. 5 . Without the ^{252}Cf source near the slabs, the singles counting rate was less than 1 cps at all HV settings showing the absence of noise in the low background in the room. With the ^{252}Cf near the detectors the singles rate increased with the “knee” at ~ 1200 V and an operating HV of 1260 V to be on the flat region of the curve. The tubes should not be operated above 1500 V because of the high gain in the tubes. The amplifier gain in the four slabs was adjusted to provide the same gain as shown in Fig. 5. The front and back slabs contain 8 ^{3}He tubes, whereas, the two side slabs contain 6 tubes each, thus, the plateaus occur at different count rates.

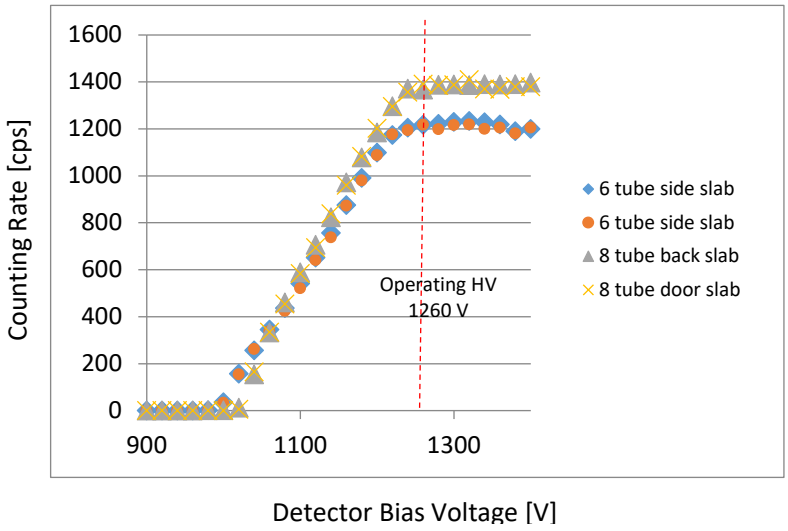

Fig. 5. The plateau curves for the four detector slabs after matching the amplifier gains to be the same.

The plateau curves in Fig. 5 were measured using a ^{252}Cf neutron source where the neutron yield is similar to the gamma yield. However, for fresh fuel assemblies the gamma emission rate is much higher than the neutron rate, so we repeated the plateau measurement using the mockup fuel assembly in the central measurement position. Figure 6 shows the corresponding plateau curve where the gamma-ray pileup counts show up at a high gain of ~ 1380 V. The operating HV of 1260 V is well below the voltage where gamma interference begins.

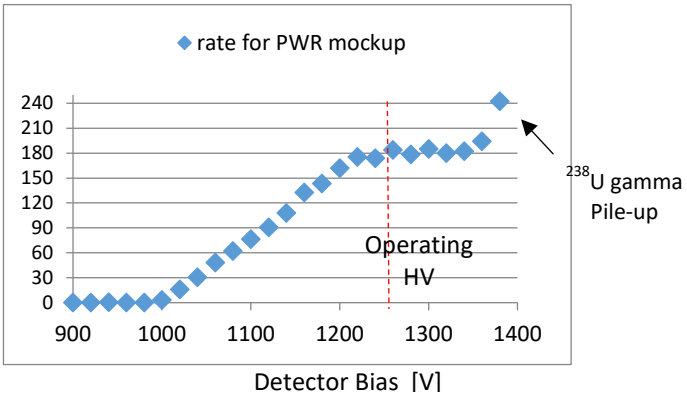

Fig. 6. The plateau curve for the sum of the four detector slabs where the source is the PWR mockup fuel assembly in the central counting position.

4.2 Response Profiles

There is a detection efficiency gradient as a function of the axial position in the fuel assembly because the collar detector geometry is open at both ends. We scanned a ^{252}Cf source along the vertical axis in the central tube of the depleted uranium (DU) mockup assembly to measure the efficiency profile that is shown in Fig. 7 (left). The ^{252}Cf source was also scanned in the radial direction with the fuel assembly

present, and the singles rate was almost flat with only a 2% increase at the assembly perimeter compared with the center.

In Fig. 7 (right), the singles rate from the passive mockup assembly is shown for the FNPC detector that was raised from near the floor up to the top of the fuel assembly that was sitting on the floor. We see that there is very little effect on the efficiency versus height until the bottom of the detector is above 60 cm from the floor. The count rate decreases at distances above 60 cm because the active region of the fuel assembly no longer completely fills the FNPC cavity. For the subsequent calibration measurements, the distance above the floor was ~ 40 cm to the bottom of the HDPE slabs.

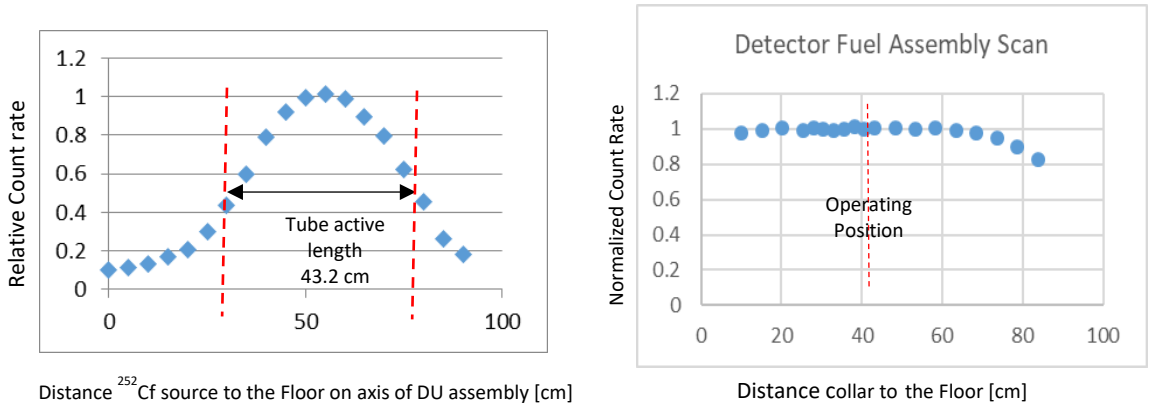

Fig. 7. The efficiency profile where the source is a ^{252}Cf source (left) and the mockup fuel assembly (right) in the central counting position.

4.3 Die-away Time

The die-away time of the detector system including the DU mockup assembly was measured using a ^{252}Cf source located in the center of the fuel assembly. The measurement method was the two gate approach where each gate pair differed by a factor of two. The resulting die-away times are shown in Fig. 8 (left) where we see that the die-away time increases as the gate time interval increases.

Because of the low counting rates for the FNPC, it is useful to increase the gate length until the accidental rate approaches the doubles rate and impacts the statistical error. The longer the gate, the larger the doubles and triples rates as illustrated in Fig. 8 (right). Because the doubles rate is a function of the fuel assembly's linear mass loading LD (g^{235}U/cm), we did measurements after loading the fuel assembly with a representative LD loading (21.9 g^{235}U/cm). With this fuel loading, our optimum gate length was determined by an analysis of the statistical error for many (1000-2000) repeat cycles of 20s each. This "sample based error" method is more accurate than alternatives such as the square root of the counts, and it is a necessity for multiplicity counting that makes use of the triples rates.

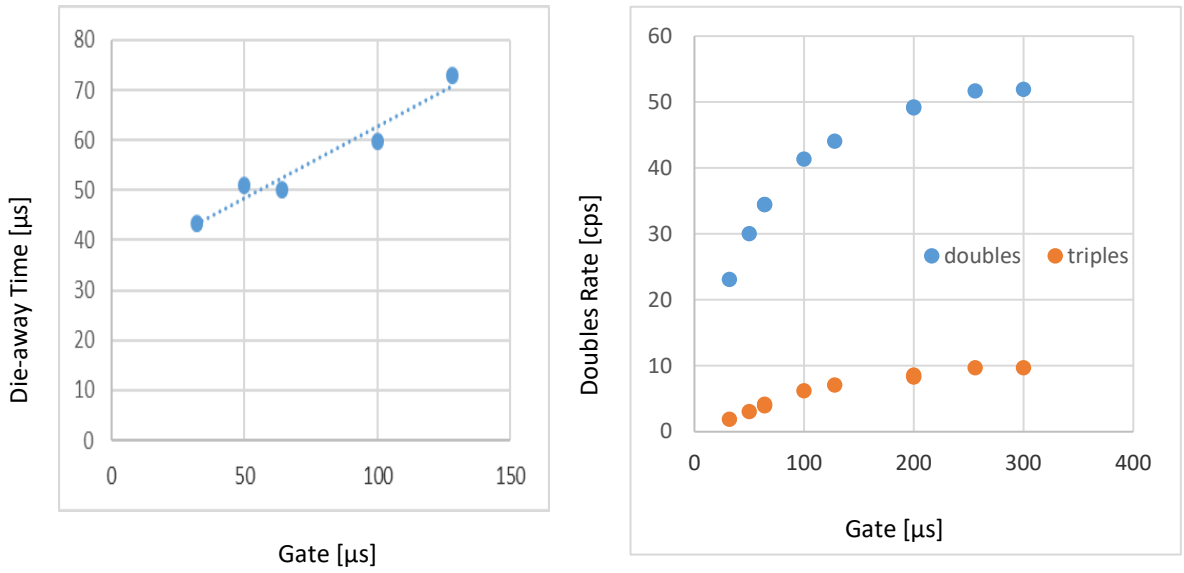

Fig. 8. The die-away times (left) and doubles and triples rates (right) as a function of the gate length where the neutron source is a ^{252}Cf source in the center of the PWR mockup fuel assembly containing DU rods.

4.4 Detector Efficiency

The detector efficiency was measured using a calibrated ^{252}Cf reference source (Cf-12) that had a neutron yield of 11,370 n/s (+/- 1.5%) on May 20, 2019. The measurements were made for the point source in the center of the empty FNPC detector both with and without the 1 mm thick Gd metal liners. The efficiency measurements were repeated with the ^{252}Cf in the center position of the mockup fuel assembly containing 204 rods to show the increased efficiency related to neutron scattering and multiplication in the assembly. Table 2 lists the measured efficiencies for the different detector conditions. The high efficiency of the passive collar is essential for the triples rates that we use for the multiplicity measurements. The key efficiency in Table 2 is the 23.9% for a point source in the center of the empty collar that can be compared with the ~ 12% efficiency for the present UNCL in the passive mode (4 slabs). The passive UNCL is used for MOX fuel assembly verification by the IAEA where the ^{240}Pu effective mass is measured.

Table 2. The efficiencies for ^{252}Cf (11,370 n/s) for different detector conditions.

Detector Status	Gate [us]	Singles [cps]	Doubles [cps]	Triples [cps]	Efficiency
Empty no Gd liners	300	2712	890.6	176.8	**0.239**
Empty with Gd liners	300	2417	734.4	129.6	0.212
Empty with Gd liners	200	2415	712.2	118.7	0.212
109 LEU rods no Gd liners	300	4077	2175.1	884.7	0.357*
109 LEU rods with Gd liners	300	3229	1247	327.9	0.284*

** Includes neutron multiplication and time correlated counts.*

6. Fuel Assembly Measurements

6.1 Mockup fuel assembly characteristics

The LANL 15x15 mockup fuel assembly shown in Fig. 3 contains 204 fuel rod positions and 21 control rod tubes (empty). The array can be loaded with all LEU rods (3.19% enriched), all Du rods (0.22% depleted) or any mixture of the two types of rods. Because of facility specific material control regulations, the loading in the low background building (TA-35, building 27) was limited to 109 LEU rods that resulted in a LD of 21.9 $g^{235}U$/cm. For subsequent measurement at a high background site (TA-66), we will increase the LD to 38.67 $g^{235}U$/cm. The fuel rod loading values that were used in the initial low background measurements are listed in Table 3. The neutron source term for the passive measurements is the ^{238}U mass that decreases as the enrichment increases, so the induced counting rates are normalized by the source term normalization shown in Table 3 to provide what we have defined as the gross counts. Normalizing to the AmLi source strength has a similar function in the present UNCL systems.

Table 3. Fuel rod loadings for the LANL calibration measurements.

LEU rods 3.19%	^{238}U rods 0.22%	Total $g^{238}U$/cm	Total $g^{235}U$/cm	^{238}U Source Norm.
0	intercept	1215	0	1.000
0	204	1210	2.66	1.004
30	174	1204	7.95	1.009
48	156	1201	11.13	1.012
59	145	1199	13.07	1.013
60	144	1199	13.25	1.013
80	124	1196	16.78	1.016
90	114	1194	18.54	1.018
100	104	1192	20.31	1.019
109	95	1190	21.90	1.021
204	0	1174	38.67	1.035

6.2 Room background

Los Alamos has an elevation of ~2200 meters above sea-level and the cosmic-ray background is more than an order of magnitude higher that for sea-level facilities. The cosmic-ray spallation background needs to be removed from the measured counts from the fuel based on the 3-sigma quality control (QC) test of the repeat measurements. The fuel assembly calibration measurements were made in a low background room that is ~ 12 m below the surface level that provides a background similar to nuclear facilities at sea-level. Prior to moving the fuel assembly into the room (TA-35, B27, R404), the singles rate was 1.0 cps and the doubles and triples rates were essentially zero. With the fuel rods in the room, the singles background was increased to ~ 1.6 cps where the 100 fuel rods were at a distance of 3.5 m from the

detector. The doubles and triples rates were < 0.01 cps for the background. Thus, for the subsequent calibration measurements, the room background was negligible (i.e. < 0.5%). For measurements in a fuel fabrication facility, the singles background is expected to be in the range of 10-40 cps and the doubles and triples backgrounds < 0.01 cps. Thus, the singles rate background would be measured and subtracted from the fuel assembly rate. The doubles and triples rates would require no room background subtraction

For our planned measurements with an average enrichment above ~ 2.0%, the detector system will be required to move to a ground-level site (TA-66) that has high backgrounds from both cosmic-rays and plutonium in a nearby storage vault. This activity is waiting for a modification in the LANL criticality regulations, and the measurement results are not included in this interim report. Our extrapolation from an LD of 21.9 $g^{235}U$/cm to an LD of ~ 60 $g^{235}U$/cm will be based on MCNP simulations.

6.3 Thermal-neutron Calibration Results

The calibration measurements were made by loading the 15x15 mockup array entirely with DU rods (204 rods at 0.22% depletion) followed by subsequent loadings of 30, 48, 60, 80, 90, 100, and 109 LEU rods as listed in Table 3. The total number of rods was constant at 204, and that provided a heavy metal loading of 1218 g/cm that is similar to typical commercial PWR assemblies (1200-1300 g/cm). The LEU rods were introduced to give a uniform distribution of the enriched rods mixed with the DU rods.

The measurements were performed using a large number of 20s cycles to provide the "sample based" error in the INCC software [7] from the data scatter. The measurements varied from 50x20s to 2000x20s to obtain high precision data with the QC 3-sigma rejection on to remove outlier events from the cosmic-ray spallation. The rejection fraction of cycles was only ~ 1.5% of the total cycles in the low background room.

The measurements included both the thermal-neutron mode (no Gd liners), and the fast-neutron mode (with 1 mm Gd liners). The pre-delay was set at 2.0 μs and the gate was 300 μs for the thermal-neutron mode and 200 μs for the fast-neutron mode. For the passive mode measurements with low counting rates, the error associated with the accidental counts is only a small component of the statistical error. The thermal-neutron mode benefited from the longer 300 μs gate because two die-away times corresponding to the initial spontaneous fission followed by the induced fission in the ^{235}U increase the lifetime of the neutrons in the detector system. The measurement results for the singles, doubles, and triples are listed in Table 4. The repeat measurements at the 3 different LD loadings (2.65, 13.07, and 21.89) were made about one month after the initial measurements to demonstrate reproducibility with respect to time, assembly position, and rod positions in the array. The average change for the repeat measurements at the 3 different LD loadings was 0.31%, 0.37%, and 1.2% for the in the measured S, D, and T rates, respectively. These differences are consistent with the counting statistical errors showing the absence of systematic errors components related to electronics drift and fuel assembly position.

Table 4. Gross and net rates for the singles (S), doubles (D), and the triples (T) for the passive FNPC with measurements in the thermal-neutron mode.

LD $g^{235}U/cm$	gross S* [cps]	gross D* [cps]	gross T* [cps]	net S [cps]	net D [cps]	net T [cps]
0	248.1	43.5	6.25	**0**	**0**	**0**
2.65	257	48.99	8.22	8.85	5.49	1.97
2.65	258.1	49.39	8.39	9.95	5.89	2.14
2.65	257.9	49.32	8.5	9.75	5.82	2.25
7.95	274	58.99	12.3	25.89	15.49	6.05
11.13	281.5	63.31	14.7	33.37	19.81	8.45
13.07	286.2	66.55	16.08	38.07	23.05	9.83
13.07	286	66.36	16.16	37.87	22.86	9.91
13.25	288	67.51	16.61	39.94	24.01	10.36
16.78	294.7	71.16	18.68	46.57	27.66	12.43
18.54	298.5	73.61	19.77	50.35	30.11	13.52
20.31	301.9	75.55	21.29	53.75	32.05	15.04
21.89	305.7	77.87	22.18	57.61	34.37	15.93
21.89	304.8	77.35	22.30	56.69	33.85	16.05

*The rates at zero g235U/cm were determined by extrapolation of the calibration curve to the zero ^{235}U mass intercept.

The gross counts include both the spontaneous fission reactions from the ^{238}U as well as the induced fission reactions in the ^{235}U and ^{238}U. The net counts correspond to the residual counts after the subtraction of the gross counts where there is zero ^{235}U mass as shown in Fig. 9 for the singles (S), doubles (D), and triples (T). The precisions for the measurements of the doubles and triples varied from 0.15-1.0% that is similar to the size of the data points in Fig. 9. We note that the maximum LD for the measurements completed to date was 21.9 g235U/cm; whereas, LD as large as ~ 60 $g^{235}U/cm$ can be expected for commercial PWR assemblies. Thus, the net counting rates will increase by more than a factor of two in going to the commercial LD loadings.

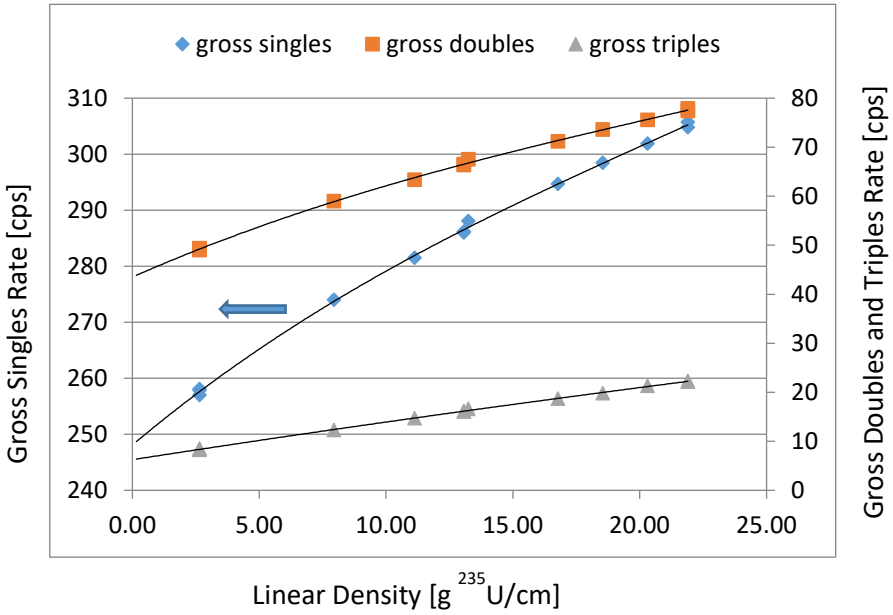

Fig 9. The measured gross counting rates for the singles, doubles, and triples as a function of the LD in the mockup fuel assembly.

Figure 10 shows the data for the net counts after the subtraction of the spontaneous fission neutrons from the ^{238}U. We see that the net ^{235}U counts are significantly less than the gross counts, and that has the effect of increasing the statistical error for the net counts. However, when the LD is increased to the loading of the commercial fuel assemblies (~ 60 g^{235}U/cm), the statistical errors are ~ 0.9%, 1.24%, and 2.04% for the S, D, and T rates, respectively for a 1000s measurement. These errors were determined via the sample based repeat counts for the multi-cycle data (see Section 8 for error details).

The net triples rates are nearly linear with a straight line through the origin, and the linearity is important as we project the triples statistical error to the ^{235}U mass error. The reason for the linear triples curve is that the thermal-neutron absorption in the ^{235}U (self-shielding) is fully compensated by the fast-neutron multiplication that increases the triples by approximately the 3rd power of the multiplication.

The statistical errors in the data for Fig. 10 are approximately the size of the data points as a result of the long measurement intervals and the stability of the detector system. Many of the measurements were made months apart after moving the detector and reloading the rod positions in the mockup fuel array. This high precision is not typical for active neutron interrogation systems because of the variability in the neutron source strengths and positioning.

Figure 10 is the most important result of the measurements in that it demonstrates a precision for the singles, doubles, and triples that is better than can be achieved with alternative measurement systems. This excellent precision makes possible the advanced analysis that solves for both the ^{235}U LD and the effective BP content independent of any operator declarations.

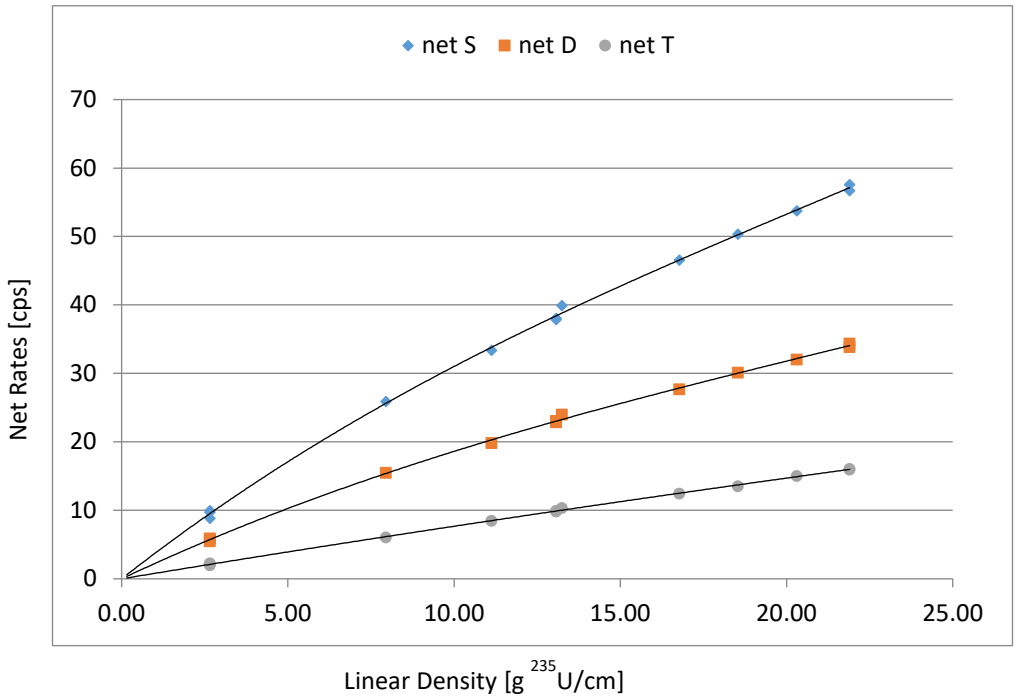

Fig 10. The measured net counting rates for the singles, doubles, and triples as a function of the LD in the mockup fuel assembly.

6.4 Fast-neutron Calibration Results

All of the calibration measurements included measurements with and without the Gd liners. The fast-neutron results are with the Gd liners to remove the thermal-neutron region of the neutron slowing-down energy spectrum. In the prior MCNP based study [4], Cd liners were compared with Gd liners and it was shown that the Gd liners reduced the perturbation from the BP rods compared with Cd liners. Thus, all of the present fast-neutron experimental measurements used 1 mm thick Gd liners.

The Gd liner mode runs were performed sequentially with the thermal-neutron mode runs listed in Table 4. Table 5 lists the fast-neutron mode data for the gross and net S, D, and T rates, respectively. The fast-neutron measurements are expected to have less dependence on the BP rod loadings than thermal mode, but at the cost of lower count rates.

Table 5. Gross and net rates for the singles (S), doubles (D), and the (T) for the passive FNPC with measurements in the fast-neutron mode.

$g^{235}U/cm$	Gross S [cps]	Gross D [cps]	Gross T [cps]	net S [cps]	net D [cps]	net T [cps]	net D+T [cps]
0.00	221.2	34.26	4.386	0	0	0	0
2.65	223.2	34.73	4.509	1.93	0.459	0.119	0.578
2.65	223.2	34.56	4.466	1.97	0.288	0.076	0.363
2.65	223.1	34.64	4.525	1.87	0.368	0.135	0.503
7.95	227.4	35.63	4.771	6.20	1.364	0.381	1.745
11.13	229.2	35.96	4.982	7.98	1.692	0.592	2.284
13.07	230.9	36.38	5.007	9.65	2.115	0.617	2.732
13.07	230.9	36.38	5.009	9.67	2.114	0.619	2.733
13.25	230.9	36.47	5.014	9.68	2.204	0.624	2.828
16.78	233.5	36.85	5.218	12.31	2.582	0.828	3.410
18.54	234.9	37.18	5.237	13.71	2.915	0.847	3.762
20.31	236.1	37.37	5.426	14.83	3.098	1.036	4.134
21.90	237.5	37.81	5.390	16.24	3.538	1.000	4.539
21.90	237.4	37.60	5.398	16.17	3.331	1.008	4.340

Figure 11 shows the plot of the fast-neutron calibration data for the gross counts for the S and D rates. We see that the induced fission rate in the ^{235}U is small compared with the spontaneous fission in the ^{238}U at the LD of < 21.89 $g^{235}U/cm$. However, at the higher LD values of ~ 60 $g^{235}U/cm$, the net rate become useable as illustrated in Fig. 12 with the linear extension to the commercial fuel loadings. The linear shapes of the three curves is a result of the hard neutron spectrum and the buildup of the ^{234}U (α, n) neutrons as the enrichment increases. The linear calibration curves are also predicted from the MCNP simulations [4].

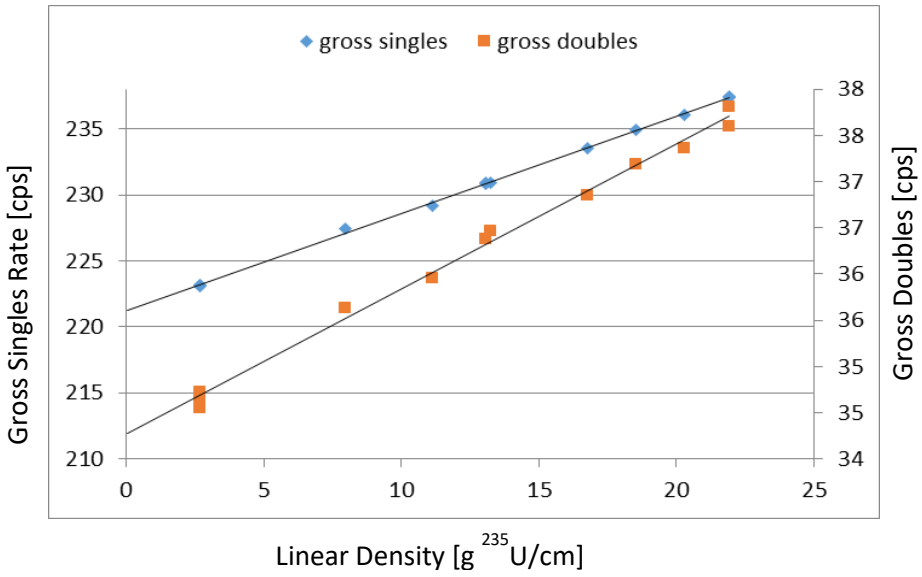

Fig 11. The measured gross counting rates for the singles and doubles as a function of the LD in the mockup fuel assembly in the fast-neutron mode.

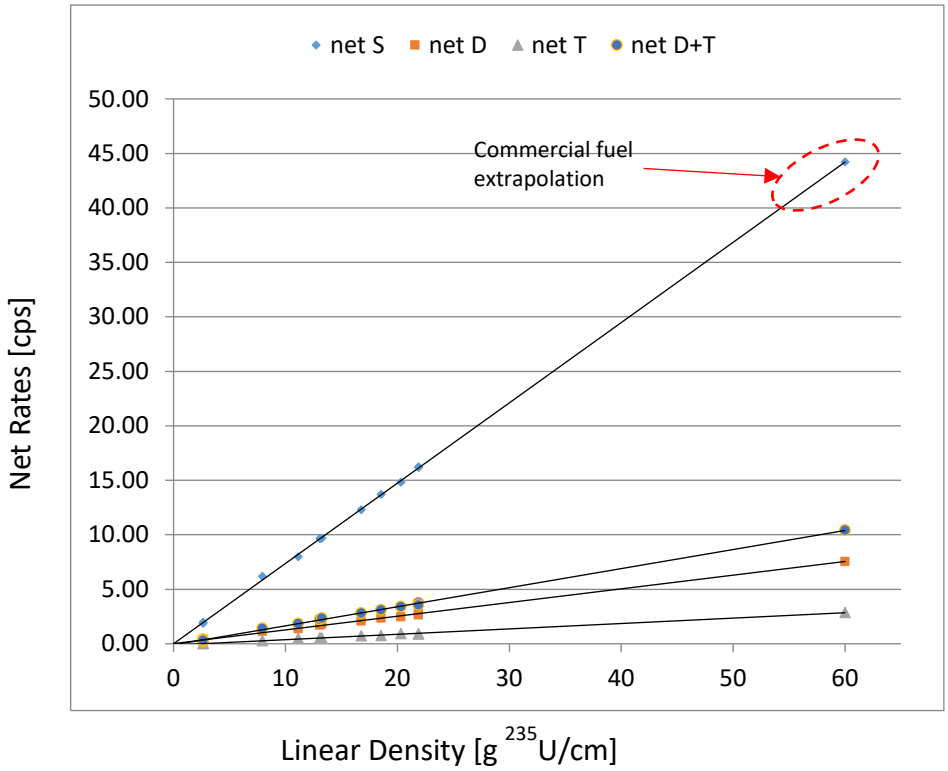

Fig 12. The measured net counting rates for the singles, doubles, and triples as a function of the LD in the mockup fuel assembly showing the calculated linear extension to a LD of 60 $g^{235}U/cm$.

Table 5 also lists the net D+T results that would represent the "Reals" in the original UNCL prior to multiplicity data collection electronics. The D+T rate with linear extension to an LD of 60 $g^{235}U/cm$ gives a net rate of 11.0 cps.

7. Burnable Poison (BP) Measurements

The effect of the burnable poisons (BP) on the original UNCL was the primary motivation for the development of the replacement collar options. The effect of the BP is much larger for thermal-neutron interrogation than for the fast-neutron (Gd Liner) case, and indeed, that was the motivation for the fast-neutron collar developments. A typical thermal-neutron interrogation system will have a BP perturbation of 20-40% on the ^{235}U measurement; whereas, for a fast-neutron interrogation (i.e. with Cd liners), the BP perturbation is reduced by about a factor of ~ 5 (3-8%). If the effect is less than this, it would indicate the lack of penetrability of the measured neutron response from the regions where the BP rods are located. The actual BP perturbation is entirely determined by the interrogation phase and not by the detection

phase. The position of the BP rods in the array changes the perturbation, and the closer the rods are to the perimeter, the larger the perturbation.

We are making use of the thermal-neutron results for our "advanced analysis" technique that solves for both the ^{235}U and the BP loading. The thermal-neutron mode increases the measured response by about an order of magnitude and provides good statistics for the S, D, and T rates. The advanced analysis uses the S, D, and T data to solve for both of the variables independent of any operator declarations, and it will be described in a separate report.

For our current measurements, we have used 12 BP rods with ~ 6% Gd2O3 loading to help evaluate the BP correction methodology in the thermal-neutron mode. These results will be presented in the separate report at the end of FY19.

8. Counting Precision and Errors

The passive mode collar was not considered in the past because of the large ^{238}U spontaneous fission component, the low counting rates, and statistical error considerations. Also, the ^{234}U (α,n) contribution was not considered at the time. The ^{238}U spontaneous fission neutron emission rate is only 13.6 n/s/kg; however, there are ~ 70 kg of ^{238}U in the active length of the passive collar, so the neutron source term is ~ 1000 n/s. The 24% efficiency would then register ~ 240 cps that is consistent with the measured singles rates in Table 4 of 257 cps for DU and 300 cps for 2% enriched LEU. The singles rate increases to > 400 cps for the commercial LD of 60 g^{235}U/cm. Also, the neutron multiplication increases with enrichment that increases the signal rates. The net singles rate for the commercial fuel would be ~ 44 cps as illustrated in Fig. 12 for the fast-neutron mode.

The statistical uncertainty in the doubles and triples is complicated by the neutron time correlations in the measured rates, and this is especially true for fast-neutron scintillation detectors. We have established the relative standard deviation (RSD) by many repeat counts of the same sample. Our measurements were performed with 50x20s to 2000x20s cycles to obtain the actual RSD. Thus, the RSD includes time correlations, electronic stability and background variations. For several of the fuel assembly loading, the measurements were made months apart and after reloading the fuel assembly, and no normalizations were required. One major advantage of ^{3}He based detector systems is that the electronic stability is good to ~ 0.01% over extended time spans of months [8].

The statistical errors for the thermal-mode system are much smaller than for the fast-neutron mode, because the net signal rates are much higher in the thermal mode. Also, the RSD errors are significantly different for the singles, doubles, and triples measurements. Table 8 summarizes the measured RSD values for both the thermal-neutron and fast-neutron modes of operation. The statistical errors are reduced by the square-root of the measurement time, so we have normalized all of the RSD values in Table 8 to a 1000s total measurement time. We note that this time is less than the typical total time for an active mode interrogation with AmLi that would include both the passive measurement plus the active measurement. In Table 8, the measured RSD values were determined at the LD loading of 21.89 g^{235}U/cm, and the RSD values at the higher loadings were calculated by extrapolating the calibration curves.

Table 8. Statistical uncertainties for 1000s based the sample based scatter from repeat measurements.

Passive Mode	Gross S RSD [%]	Gross D RSD [%]	Gross T RSD [%]	Net S RSD [%]	Net D RSD [%]	Net T RSD [%]
Thermal-Neutron Mode						
LD @ 21.9 g^{235}U/cm	0.23	0.73	2.69	1.65	2.69	3.73
LD @ 36 g^{235}U/cm	0.214	0.67	2.2	1.27	1.97	2.89
LD @ 60 g^{235}U/cm	0.198	0.61	1.71	0.89	1.24	2.04
Fast-Neutron Mode						
LD @ 21.9 g^{235}U/cm	0.241	0.795	3.75	3.73	9.39	22.10
LD @ 36 g^{235}U/cm	0.231	0.654	3.02	2.43	6.41	15.06
LD @ 60 g^{235}U/cm	0.221	0.514	2.26	1.12	3.43	8.01

The key values in Table 8 correspond to the commercial PWR LD loadings of ~ 60 g^{235}U/cm where the errors (1-sigma) are below ~ 2.0% for the thermal mode. The errors are all based on repeat measurements that were typically 2000x20s. If the doubles error were calculated via the square-root of the doubles plus accidental counts, the error would be a factor of ~ 1.5 smaller than the values in Table 8. The sample based errors are larger because the doubles and triples rates are correlated in time.

In the fast-neutron mode, we would propose using the singles rate as the primary assay result, and the net doubles rate as confirmatory information because of the 3.43% statistical error. The triples rate would not be used for the fast-neutron mode because of the large statistical error. However, the linear shape through the origin of the net singles and doubles calibration curves means that the net errors are the same as the ^{235}U mass errors and are below the ITV target values [9] for the singles and doubles measurements. Thus, both the singles and doubles accuracies meet the ITV criteria for the UNCL as applied to fresh LEU fuel assemblies.

In the thermal-neutron mode, all three observables (S, D, and T) can be used to solve for both the ^{235}U and the effective BP loading. The statistical error for the ^{235}U mass is below 2%, and the errors will be quantified in a separate report on “Advanced Analysis”.

9. Fuel Assembly Mass Effect

The fuel assembly mass and size effects the measurement results because neutron scattering and the form factor (positioning) inside the neutron collar. Commercial PWR fuel assemblies typically have a 17x17 rod matrix, but there are older reactors that use 14x14 (etc.) rod arrays. Also, many of the new reactors have the WWER-1000 hexagonal rod array. The original UNCL made a calibration correction for the heavy metal linear density change called the k_4 correction to the doubles rate in the INCC code. For the passive collar there are two approaches to account for the change in assembly type and size; 1) introduce k4 type corrections for the singles, double, and triples; or 2) introduce separate “material type” categories in the calibration files of the software. For the IAEA verification of plutonium samples, there are different material types to for the different sample categories, and the INCC code carries the corresponding calibration coefficients.

10. Summary

This report provides the detector parameters, performance measurements, and preliminary calibration of the fast-neutron passive collar (FNPC) that is used to measure the ^{235}U linear density in PWR type fuel assemblies. The current development is unique from prior systems that are used to verify the ^{235}U content in fuel assemblies in that it does not require the use of an external interrogation source such as AmLi. The self-interrogation is accomplished by using the ^{238}U spontaneous fission neutrons to induce the fission reactions in the ^{235}U that coexists in the same fuel pellets. This uniform neutron source distribution also provides a more uniform interrogation as a function rod position compared with exterior interrogation sources.

The measured neutron efficiency of the FNPC is 24% for a ^{252}Cf source located in the center, and that is significantly higher than prior neutron collar systems. The UNCL in the passive mode (i.e. 4 sides) is ~ 12% efficient. The high efficiency for the FNPC provides useful statistical results (1-2%) in measuring times of 600-1000s for the net singles rate in the fast-neutron mode. The doubles precision was 3.43% in the fast-neutron mode and 1.24% in the thermal-neutron mode. Because of the linear shape of the net fast-neutron results (see Fig. 10), the RSD % error for the net rates and the ^{235}U mass % error are approximately the same. In the thermal-neutron mode the net rates have RSD values below ~ 2.0%.

The system has been calibrated in both the fast-neutron mode (Gd liners) and the thermal-neutron mode (liners removed). Calculations using the MCNP code have shown that the 1mm thick Gd liners reduce the BP perturbation more than for 1 mm thick Cd liners that are typically used [2]. The purpose for the fast-neutron mode is to minimize the perturbation from the BP rods in the fuel assemblies. As an alternative to the fast-neutron mode, the thermal-neutron mode provides good doubles and triples statistical precision to solve for both the ^{235}U and BP content. The high efficiency makes multiplicity counting practical and analysis that makes use of singles, doubles and triples rates where the triples rates have not been available in prior collar systems.

The preliminary evaluation of the advanced analysis capability to independently solve the multiplicity data (singles, doubles, and triples) for both the ^{235}U mass and the effective burnable poison content (regardless of the BP rod configuration) showed good potential. All other fast-neutron collar type measurement systems have a 3-10% residual correction in the ^{235}U mass related to the poison rod perturbation and rod locations. For the AmLi interrogation systems, the error in the ^{235}U LD is larger than the error in the doubles rate because of the calibration curve shape. The present multiplicity analysis method is the only neutron based measurement approach that is truly independent of the poison rod problem. Also, for some assembly verifications prior to shipping, control rods are in the assemblies in addition to BP rods for criticality control, and the advanced analysis can handle this condition; whereas, the fast-neutron systems cannot.

The passive system is less complex than the alternative active-neutron interrogation systems, and that makes the potential unattended mode application more practical. The unattended mode would have the advantage of reducing the inspection time for IAEA verification of the fresh fuel assemblies. Experiments

and analysis to help evaluate the unattended mode of operation will be presented in a separate report [10] under this project (24.1.3.1, Task 4).

11. Acknowledgements

The authors would like to thank the NNSA's Office of International Nuclear Safeguards (NA-241) for the funding for this work.

12. References

[1] Menlove, H. O., et. al. "Neutron Collar Calibration and Evaluation containing Burnable Neutron Absorbers", Los Alamos National Laboratory Report, LA-11965-MS, (1990).
[2] UNM Rodeo-II paper from 2019 INMM Annual Meeting (2019).
[3] Root, M. A., et al. "Using the Time-Correlated Induced Fission Method to Simultaneously Measure the 235U Content and the Burnable Poison Content in LWR Fuel Assemblies." *Nuclear Technology*, 2018, pp. 1–14.
[4] Margaret Root, William Geist, Anthony Belian, and Howard Menlove, "Fast Neutron Passive Collar Project Year End Report". Los Alamos National Laboratory Report, LA—UR-18-29560, (2018).
[5] JSR-15 Shift Register electronic module produced by Canberra Industries, Meriden, CT. www.canberra.com/contact
[6] Mathew Newell, advanced list mode module (ALMM), private communication January (2019).
[7] W. Harker, M. Krick, and J. Longo "INCC Software Users Manual," Los Alamos National Laboratory document LA-UR-01-6761 (rev) (November 2005).
[8] D. Henzlova, et. al. "Results of the Evaluation and Comparison of Alternative Neutron Detectors for Potential 3He Replacement for Nuclear Safeguards Applications", Los Alamos National Laboratory Report, LA-12-00837, (2012).
[9] International Target Values 2010 for Measurement Uncertainties in Safeguarding Nuclear Materials, ESARDA Bulletin, Number 48, ISSN 0393-3029 (2012).
[10] Root, LA-UR unattended mode report in preparation, (2019)